

Controlling and Assessing the Surface Display of Cell-Binding Domains on Magnetite Conjugated Fluorescent Liposomes

Dewi Harjanto,[†] Joosub Lee,[‡] Jong-Man Kim,^{‡,§} and Justyn Jaworski^{*,‡,§}

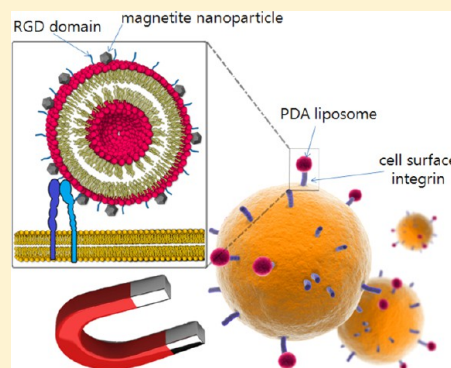
[†]The Rockefeller University, 1390 York Ave, New York, New York, United States

[‡]Hanyang University, 222 Wangsimni-ro, Seongdong-gu, Seoul, South Korea

[§]Institute of Nano Science and Technology, 222 Wangsimni-ro, Seongdong-gu, Seoul, South Korea

S Supporting Information

ABSTRACT: Biological systems provide us with a diverse source of peptide-based ligands for cellular adhesion. Controlling and assessing the ligand surface density as well as tailoring the surface chemistry to have specific cellular adhesion properties are important in biomaterials design. In the following work, we provide a means for displaying peptide-based ligands on magnetic liposomes in which the surface density and chemistry may be controlled. Simultaneously, the conjugated vesicles provide a fluorescent signal for examining steric hindrance among surface ligands. In addition, the inherent magnetic and fluorescence features of this system revealed potential for magnet-based cell isolation and fluorescent labeling of adhered cells, respectively. Adhered cells were found to remain viable and proliferative, thereby allowing them to be used for subsequent evaluation. In a specific demonstration, we control the density of fibronectin-mimetic ligands on the polydiacetylene liposome surfaces. We find that steric limitation occurring at over 20% surface density result in decreased cell adhesion, in accord with related techniques. The magnetic-liposome system offers the means for not only separating cells adhered to the biomaterial, but also providing the ability to control and assess the biomaterial surface. This may prove particularly useful for examining combinations of peptide-based ligands or for evaluating the molecular-level ligand accessibility and its effect on cell attachment to a biomaterial surface.



■ INTRODUCTION

During cell migration and numerous other physiologically critical processes, cell adhesion receptors, such as integrins, form complexes with the surrounding environment, including foreign surfaces (biomaterials), extracellular matrix materials, as well as other cells.¹ Directing cell fate through controlled surface interactions is one of the key approaches used in biomaterials engineering. Control of ligands displayed on a biomaterial in terms of surface density and surface chemistry can thus greatly affect cell adhesion capabilities. The crosstalk occurring at the cell–biomaterial interface entails a number of factors including topographical and mechanical effects as well as biological cues.² As such, there remains practical need for a system that may help to deconvolute the effects of chemical surface signals on cell adhesion. Cell adhesion assays have been developed that are working in this direction in order to quantify the capability of cells to bind to a given biomaterial surface. In vitro cell adhesion assays are designed to mimic in vivo conditions in a more controlled manner in order to assess a biomaterial's interaction with a given cell type.³ In conventional cell adhesion assays, cells that have bound to a treated biomaterial surface of interest are detected using a dye, enzymatic assay, radioisotope, or intracellular fluorescence, after washing the surface to remove nonadherent cells.⁴ In these approaches, often an inherent bias exists in the generated signal

as it highly depends on the cell line used, and moreover there is an unfortunate requirement for cell lysis in dye and enzymatic-based detection,^{5,6} which may prevent further assessment of cell function. Assessment of cell function is a crucial requirement if we are to gain a better understanding of how biomaterial interactions ultimately affect the cells behavior and eventual fate. Hence, there remains a need for a system wherein the surface properties may be both easily tailored and assessed, while remaining nondestructive to the cell such that their behavior may be further probed by subsequent analytical methods.

In this work, we put forth an approach for controlling the surface density of cell adhesion ligands displayed on the surface of magnetically functionalized liposomes (Figure 1). In addition, the native fluorescence and magnetic properties of the functionalized liposomes demonstrate value for assessment of the biomaterial surface and for cell separation, respectively. Magnetic liposomes have been employed extensively in the past in a variety of biomaterials applications, including use as a carrier for drugs or in conjunction with antibodies for selective labeling of target cells.⁷ Drug-loaded magnetic liposomes

Received: February 11, 2013

Revised: May 7, 2013

Published: May 14, 2013

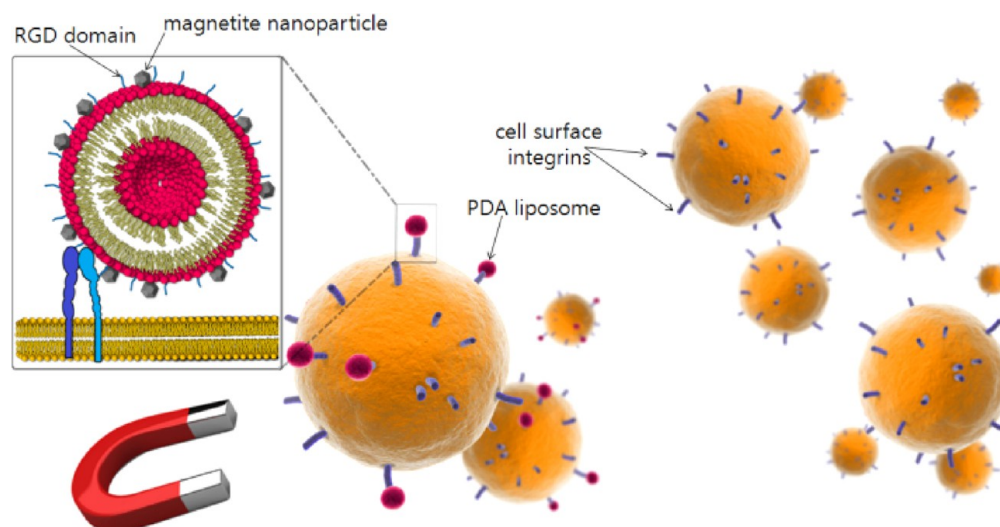


Figure 1. Overview of magnetite labeled PDA liposomes capable of binding to cell surface integrins by the controlled display of RGD ligands. This system allows control over the surface density and chemistry of displayed ligands, allows for fluorescent assessment of surface steric affects, and offers a technique for screening of a biomaterial's cell adhesivity.

coated with the peptide Arg-Gly-Asp (RGD) have been shown to be taken up by neutrophils and monocytes for drug delivery to the brain, as these cells are able to breach the blood–brain barrier.⁸ In addition, injected magnetic liposomes have been successfully guided to target tumor sites for enhancement of magnetic resonance imaging.⁹ It follows that magnetic liposomes have also been engineered to possess RGD motifs for cell binding. Researchers have shown that such a system may be used for the reversible formation of cellular sheets capable of detachment by magnetic release for tissue engineering application.¹⁰ In our work, we present a magnetic liposome-based platform which offers control over surface density and surface chemistry for the study of cells in vitro. Herein, we reveal that cells adhered to RGD functionalized magnetic liposomes can be easily separated for counting using an ordinary hemocytometer and subsequently used for further assessment of the biomaterials affect on cellular behavior. In this approach, the fluorescent properties of the liposome offer a unique means for assessing steric affects at the biomaterial surface, thereby providing information useful in the design of ligands and interfaces for cell-biomaterial interactions.

The ligand presented on our liposomes is the peptide sequence Arg-Gly-Asp (RGD). This short peptide motif is an extracellular matrix (ECM) domain found in many cell adhesion proteins, including fibronectin, vitronectin, and fibrinogen, and is recognized specifically by $\alpha 5 \beta 1$ integrins; hence, it is widely used in biomaterials applications for cell adhesion.^{11,12} We too chose to implement RGD, since peptide chemistries can be easily integrated onto our liposomes by solid phase peptide synthesis. Due to the self-assembling nature of the polymeric liposomes, we could specifically control the display of various surface densities of the ligand, RGD. The self-assembly arises from the main structural component of the vesicle, which is the amphiphilic monomer, 10,12 pentacosyldioic acid (PCDA). After simple solid phase peptide synthesis of RGD, the PCDA motif was capped onto the exposed free terminal amine. Cleavage from the solid phase resin affords the amphiphilic monomer, referred to here as PCDA-RGD, which is used to control the density of the displayed ligand during liposome formation. Full details on the

synthesis of PCDA-RGD are provided in the Supporting Information, SI, whereas a detailed schematic of the PCDA and PCDA-RGD structure can be found in (Figure 2). By dissolving

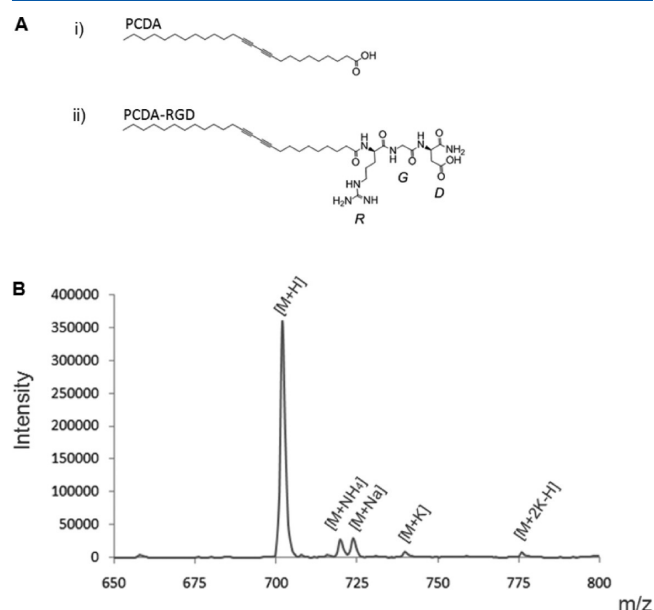


Figure 2. (A) Chemical structure of liposome constituents, (i) PCDA and (ii) PCDA-RGD, used during liposome self-assembly. (B) MALDI-TOF spectrum of synthesized PCDA-RGD.

PCDA (containing no peptide headgroup) and PCDA-RGD in DMSO at specific molar ratios of 100:0, 95:5, 90:10, 80:20, and 50:50 followed by injection into aqueous buffer, we could control the proportion in which the self-assembled mixtures would form into liposomes, thereby allowing specific surface densities of the RGD peptide. Brief exposure of the liposomes to UV light facilitated polymerization of the PCDA/PCDA-RGD diacetylene monomers, resulting in stabilization of the liposome structure for a given surface density of RGD. In addition, this UV exposure simultaneously sterilizes the material, which is a necessity in cell culture applications. The

liposomes reveal a hydrodynamic diameter of 93 nm by dynamic light scattering (Supplementary Figure 1 of the SI), which is in agreement with typical PDA liposomes.¹³

The UV polymerized form of PCDA, referred to as polydiacetylene (PDA), has been widely studied for sensing applications due to its responsiveness to temperature and mechanical force, among other stimuli.^{14–16} Upon stimulation, the material changes color from a blue phase to a fluorescent red phase. Also contributing to the popularity of PDA is its ability to self-assemble into highly ordered supramolecular structures, including liposomes and nanotubes.^{17–19} In the past, diacetylene derivatives have been functionalized with amino acid sequences to produce peptide amphiphile-based liposomes capable of binding to selective targets such as small molecules and proteins, including integrins.^{20,21} Although PDA has received limited attention for cell studies,^{22,23} it has been shown that murine fibroblasts could adhere and spread on 2D PDA films functionalized with fibronectin derivatives.²³ With this in mind, we explored the potential for assessing cell adhesivity to controlled biomaterial surface coatings for magnetic PDA liposomes.

PDA magnetic composites have recently been developed for sensing applications.^{24,25} We too have revealed that magnetite nanoparticles could be easily functionalized to the terminal carboxylic acid site of PDA liposomes through simple sonication.²⁶ The integration of magnetite onto other biomaterials of interest that contain a terminal carboxylic acid site, such as polylactic acid or polyglycolic acid is therefore conceivable. Our strategy was used to yield magnetite-functionalized PDA liposomes possessing controlled RGD densities. The 20 nm diameter magnetite nanoparticles used in this work are smaller than the single-domain limit and experiments were conducted well above the blocking temperature, suggesting super paramagnetic behavior rather than ferrimagnetism for our nanoparticles.^{27–29} From a practical perspective, this allows for the nanoparticles to aggregate for collection under an applied magnetic field and redissolution when the external field is removed. The hydrodynamic diameter of magnetite labeled liposomes containing 20% PCDA-RGD was found to be approximately 0.4 μm , confirming our prior work that the magnetic-liposomes can exist as clusters or aggregates. SEM and TEM images reveal the manner in which the outer surfaces of the liposomes are decorated with magnetite nanoparticles having a diameter of approximately 20 nm. After the liposomes were functionalized with magnetic nanoparticles, the magnetic liposomes were used to demonstrate that the controlled biomaterial surface could provide cell-adhesion sites and subsequently be used to magnetically separate cells from the solution. In brief, we may separate cells by first incubating them with the magnetic liposomes in a tube containing serum-free media and then collect bound cells by applying a magnet to the outside of the tube. After washing, the number of cells adhered to the biomaterial can be quantified using a standard hemocytometer to provide the relative cell adhesion ratio to assess adhesivity. From cytotoxicity studies (Supplementary Figures 3 and 4 of the SI), we observed that an increasing amount of these magnetic liposomes can result in decreased cell viability; however, at the concentration relevant to our cell separation study the cells remain viable offering the potential for subsequent analysis of the biomaterial's effect on cell behavior.

In this study, we find that the magnetic liposomes may be rapidly and easily customized in terms of ligand chemistry and

surface density. In addition to providing a means for quantifying steric hindrance among ligands for different surface densities on the liposome surface, we also found the potential of assessing the cell adhesion capabilities via magnetic separation. This work may have relevance to researchers working in cell sorting, biosensing, targeted therapeutics, or imaging applications. Herein, we provide further discussion on the use of the magnetic liposomes for evaluating the surface sterics associated with increasing surface densities of displayed RGD and the corresponding effect on cell adhesion. In addition, we provide our analysis of the separation capabilities of the system and discuss its potential as a nondestructive platform for probing cell adhesivity with respect to biochemical surface cues.

■ EXPERIMENTAL SECTION

Solid-Phase Synthesis of PCDA-RGD. Arg-Gly-Asp functionalized diacetylene monomers, 10,12-pentacosadiynoic-acid-arginidyl-glycidyl-aspartidyl (PCDA-RGD), were synthesized using standard solid-phase peptide synthesis via Fmoc chemistry.³⁰ Full experimental details are provided in the SI.

Characterization. To verify that the desired product was synthesized, ¹H NMR and MALDI were performed using the lyophilized product. The ¹H NMR data were collected on a Mercury Plus 300 MHz instrument using DMSO-*d*₆ as the solvent. ¹H NMR (300 MHz, DMSO-*d*₆, δ): 8.45 (m, 1H, CNHNH₂ Arg), 8.03–8.07 (m, 3H, CONH Arg, Gly, Asp), 7.16 (s, 2H, CONH₂ Asp), 4.4–4.35 (m, 1H, α -CH Asp), 4.25–4.2 (m, 1H, α -CH Arg), 3.8–3.7 (m, 2H, α -CH₂ Gly), 3.1 (m, 2H, β -CH₂ Asp), 2.78 (s, 1H, δ -CH₂ Arg), 2.22–2.32 (m, 4H, CH₂C \equiv C PCDA), 2.18–2.1 (d, 2H, CH₂C=O PCDA), 2.0 (m, 1H, NH Arg), 1.8 (m, 2H, β -CH₂ Arg), 1.45 (m, 2H, γ -CH₂ Arg), 1.41 (m, 6H, CH₂ PCDA), 1.25–1.15 (m, 16H, CH₂ PCDA), 1.15–1.05 (m, 10H, CH₂ PCDA), 0.82 (t, 3H, CH₃ PCDA). Mass spectroscopy was performed using a Shimadzu Axima Performance MALDI-TOF operating in linear mode with sample mixed in α -cyano-4-hydroxycinnamic acid (CHCA) matrix. Dynamic Light Scattering (DLS) was also performed in order to characterize the size of the liposomes and magnetite-conjugated liposomes. The dynamic light scattering (DLS) data was collected using a Malvern ZEN3600. Scanning electron microscope (SEM) images were obtained using a JEOL (JSM-6330F) microscope, and samples were coated with platinum for 15 s prior to analysis. Transmission electron microscopy (TEM) images were recorded using a JEOL JEM-2100 (performed at 120 kV).

Liposome Formation, Polymerization, And Magnetite Conjugation. Liposomes were formed as previously described,²⁶ with varying PCDA-RGD:PCDA content. Briefly, PCDA-RGD and PCDA were dissolved in 200 μL DMSO before being added to 15 mL HEPES (10 mM, pH 7.4) which was previously heated to 80 $^{\circ}\text{C}$ in a water bath. The sample was tip-sonicated for 15 min, and then filtered through a 0.8 μm filter while warm. The liposomes were placed in a 4 $^{\circ}\text{C}$ fridge overnight to facilitate liposome formation. The samples were then polymerized for 30 min at a distance of 5 cm using a hand-held UV lamp (254 nm). The 1 mM liposome samples were constructed with a PCDA-RGD content of 0, 5, 10, 20, and 50%. Samples were stored at 4 $^{\circ}\text{C}$. UV-vis and fluorescence spectra of samples diluted to 0.167 mM in HEPES buffer were recorded with observation of temperature effects on the liposome optical properties in order assess steric hindrance of PCDA-RGD incorporated in the liposomes. Liposomes were conjugated to magnetite using our previously established protocol.²⁶ In brief, a 1 mM acidic solution of magnetite in distilled water was prepared by sonication in water for 20 min, and adding aqueous HCl to bring the pH down to 2.0. Next, 1 mL of the 1 mM mixed lipid solution was added to 8.75 mL of distilled water, followed by 250 μL of the magnetite solution. The pH was adjusted to 3.6 with HCl prior to additional sonication for 3 min. The magnetic-liposomes were then concentrated using a neodymium magnet and resuspended in 10 mM HEPES buffer pH 7.4 to a concentration of 40

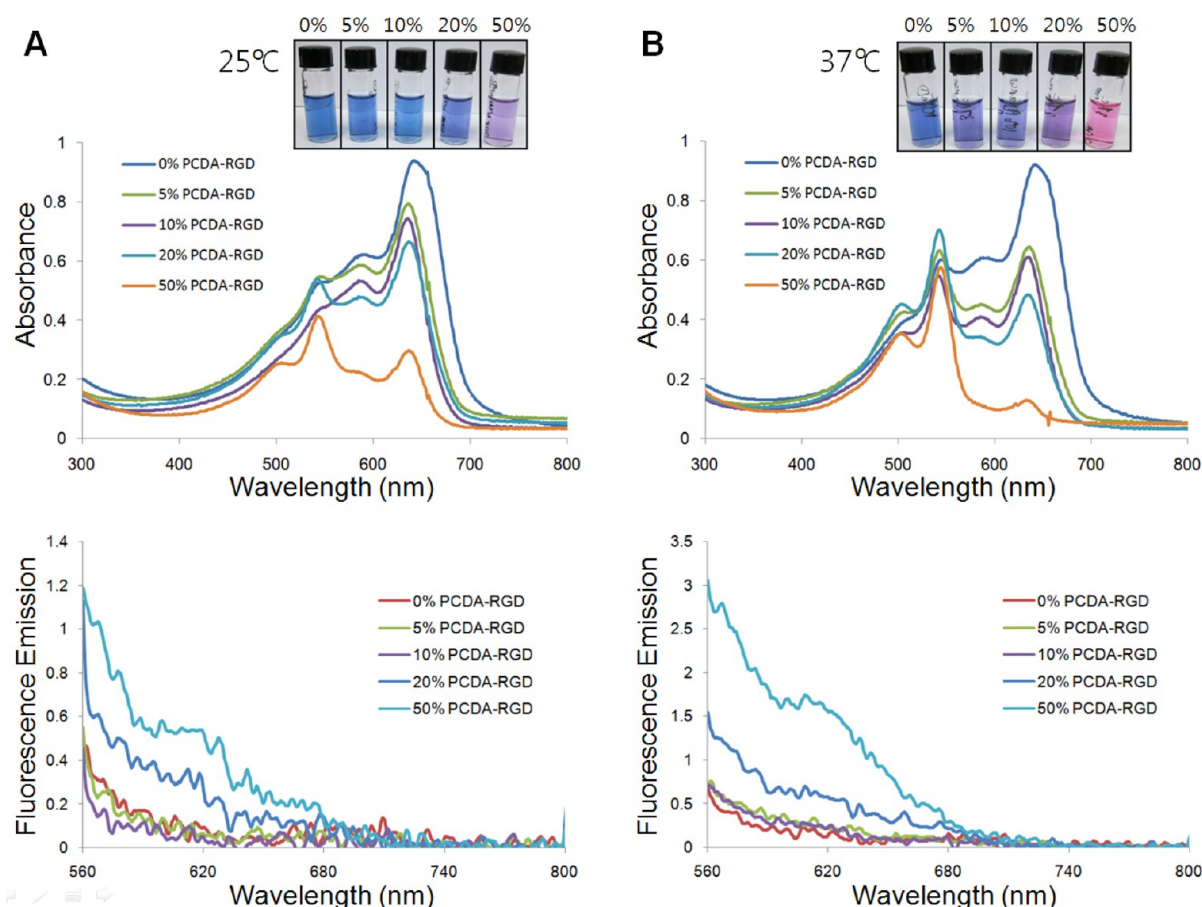


Figure 3. Effect of temperature (A) 25 °C and (B) 37 °C as well as PCDA-RGD surface sterics as assessed by the colorimetric and fluorometric properties of liposomes in aqueous solution. (Top) Photograph of vials containing 0.167 mM liposomes composed of 0, 5, 10, 20, and 50% PCDA-RGD, respectively. (Middle) UV-vis absorption spectra and (Bottom) fluorescence emission spectra (540 nm excitation wavelength) of corresponding vials from the top photo.

mM magnetic-liposomes with respect to the amount of mixed lipid content. The samples were then stored at 4 °C.

Cell Culture. NIH 3T3 cells obtained from Prof. Hee Yong Chung at Hanyang University were cultured using standard cell culture techniques. The cells were nourished with DMEM, 1% v/v penicillin/streptomycin, and 10% v/v newborn calf serum, and maintained in an incubator at 37 °C, 5% CO₂ with passaging every 2–3 days when reaching 80% confluence.

Cytotoxicity Study. The effect of magnetic liposomes containing 20% RGD on the viability of 3T3 fibroblasts was assessed by 24 h growth of cells in the presence of various concentrations of the magnetic liposomes at 37 °C. After 24 h of exposure, the mitochondrial reductase activity of viable cells was assessed using 3-(4, 5-dimethyl-2-thiazolyl)-2, 5-diphenyl-2H-tetrazolium bromide at a final concentration of 2 mg/mL in 1:1 DMEM:PBS and incubation for 3 h at 37 °C followed by removal and dissolution of the resulting purple MTT formazan crystals by addition of isopropanol containing 4 mM HCl and 0.1% IGEPAL CA-630 (Sigma Aldrich). The extent of cell viability was assessed by comparison of the absorbance ($A_{595}-A_{650}$) of magnetic liposome exposed samples and controls. Samples transferred to 96-well plates were analyzed on a Molecular Devices E-Max microplate reader with data obtained using SoftMax Pro 5.4.

Cell Adhesion Study. A 5- μ L portion of 40 mM magnetic liposome solution was added to 250 μ L suspensions of NIH 3T3 cells (at 2.25×10^7 cells mL⁻¹) in serum-free DMEM media in a 5 mL round-bottom polystyrene tube, and incubated for 15 min at 25 °C. Next, 2.5 mL of media was added before applying a neodymium magnet for 10 min at room temperature. The tube was then inverted for 3 s to remove unbound cells, and 2.5 mL of fresh media was added to the tube. The tube was again exposed to the magnet for 10 min to

repeat the washing steps a total of 5 times. After the final rinse, the cell suspension volume remaining in the tube was determined, and the total number of bound cells was determined using a hemocytometer. The cell adhesion ratio was calculated as the figure of merit for the adhesivity as the number of cells transferred after magnetic separation and washing relative to the number of cells in the original solution. In doing so, we can provide a quantitative measure of adhesiveness to a liposome of a given biomaterial composition. Liposome-bound cells were then plated onto cell culture dishes. Experiments were performed in triplicate.

Cell Microscopy. Imaging was performed on magnetically separated cells 1 h after isolation and 1 day thereafter, using an inverted microscope (Olympus IX71). Microscopy was done using 20 \times and 40 \times objectives, with both phase contrast and a Texas Red filter set. ImageJ (NIH, U.S.) was used for overlaying the images.

RESULTS AND DISCUSSION

After controlled proportioning of the PCDA and PCDA-RGD monomers for self-assembly and subsequent UV polymerization, the resulting liposomes could immediately be observed to have a distinct color difference as a function of the RGD ligand surface density. Liposomes with a low ligand surface density exhibited the typical blue phase [UV-vis (water): λ_{\max} = 626 nm], while increasing ligand surface densities resulted in an increasingly triggered red phase [UV-vis (water): λ_{\max} = 536 nm], which display a concomitant red fluorescence (Figure 3). This red phase shift has been attributed to steric hindrance due to adjacent RGD ligands, thereby resulting in breaking of the π -

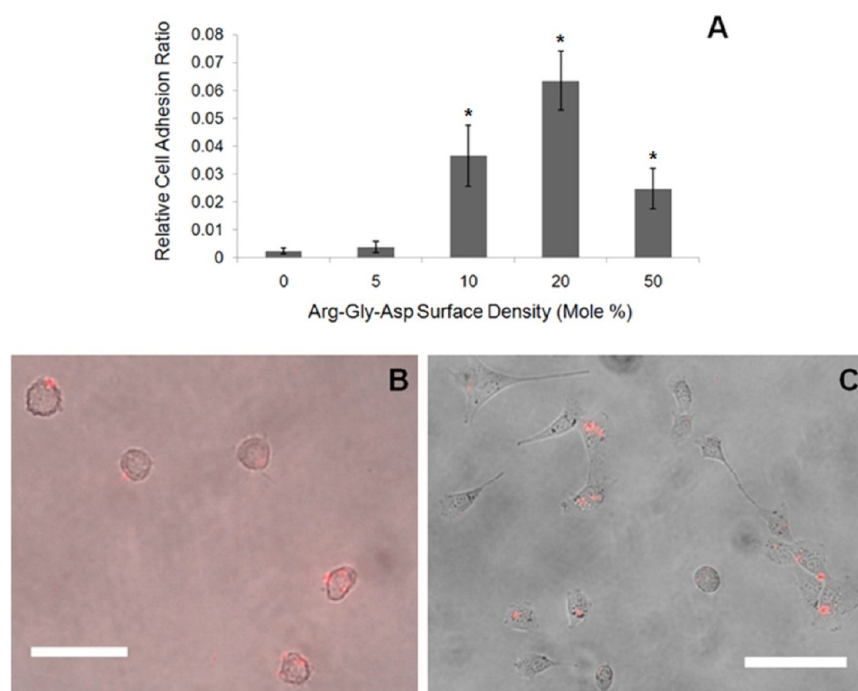


Figure 4. (a) Relative cell adhesion ratio to liposomes of varying PCDA-RGD content as determined by magnet-based cell separation ($n = 3$, * represents data having a p -value < 0.01 by two-tailed t test relative to the 0% RGD condition). (b) Cells attached to 20% PCDA-RGD liposomes (red) 1 h after separation. Note that the liposomes are mostly at the cell edges. Scale bar: 50 μm ; (c) cells attached to 20% PCDA-RGD liposomes (red), showing spread, normal morphologies 1 days after cell separation. Scale bar: 100 μm .

π backbone planarity of the conjugated diacetylenes.²¹ An additional consideration in this work is our incorporation of magnetite nanoparticles on the exterior of the resulting liposomes. The use of spacer segments between fluorophore and magnetite domains in hybrid systems have been suggested to reduce the possibility of fluorescence quenching by magnetite.^{31,32} In this work as well, the fluorescent PDA backbone, which exists in the middle of the assembled structure, has a 10 carbon chain spacer to the exterior oxygen species, which may provide the necessary distance for us to continue observing the liposome fluorescence when attached with magnetite. Observation of the colorimetric and fluorescent properties, as well as the structural features of the liposomes, has previously revealed that no significant deformation results from attachment of the magnetic nanoparticles.²⁶ In the same prior study, the use of higher concentrations of magnetite was found to result in the formation of progressively larger aggregates of the PDA-magnetite hybrid. In this work, aggregates having a hydrodynamic radius of approximately 0.4 μm were used for cell adhesion studies (Supplementary Figure 1 of the SI). In our evaluation of the effect of ligand surface density on the cell adhesion capability, magnetic liposomes bearing a range of surface densities of RGD, from 0 to 50%, were implemented. NIH 3T3 cells were exposed to the peptide coated magnetic liposomes for 15 min to allow interactions between the adhesion ligands and the cells' integrins. Since the magnetic-liposomes exist as aggregates, the cells observe individual clusters of several magnetic-liposomes bearing adhesion ligands rather than merely a single isolated liposomes. As a result of such collective effects, the simple external magnet may more strongly attract the clusters in contrast to isolated particles. After collection by magnet, the unbound cells were removed, and the suspension was washed with fresh media. This was repeated five times in order to eliminate unbound

cells, and the resulting bound cells were counted using a hemocytometer. This entire procedure was repeated in triplicate for each of the various surface densities of RGD. The relative cell adhesion ratio for each of these conditions is reported in Figure 3. From these results, we could determine the optimal surface density for cell adhesion to our biomaterial was 20% surface density of RGD. This reasonably reflects the trade-off between the multivalent nature of integrin mediated cell adhesion (positive correlation to cell adhesion) and the steric limitations created by an overly dense number of ligands on the surface (negative correlation to cell adhesion). Above 20% surface density, we found the extent of cell adhesion decreased significantly. Interestingly, we found these results coincide with a report from another group showing that a 20% surface coating density of fibronectin-mimicking peptide ligand (similar to the RGD used in our study) on a 2-D Langmuir–Blodgett film provided improved binding to an integrin immobilized surface compared to higher ligand surface density.³³ To examine if the effects were arising rather from the perceived surface charge, a chemical moiety (EDEA, 2,2'-(ethylene dioxy)-bis-(ethyl amine)) was conjugated to PCDA and examined for its cell adhesion capability. As PCDA-EDEA contains a primary terminal amine with correspondingly similar length and net surface charge distribution as PCDA-RGD, it was tested as a comparison also at 20% surface density (Supplementary Figure 6 of the SI). Results of magnet-based cell separation using 20% surface density of EDEA revealed no significant difference from the case of 0% surface density suggesting the importance of complex surface chemistry (i.e., amino acid residues) on biomaterial adhesion.

Given the fluorescence of PDA, we were also able to directly assess the occurrence of any surface group steric hindrance from colorimetric/fluorometric data (Figure 3). Before any cell attachment or magnetite functionalization, the PDA liposomes

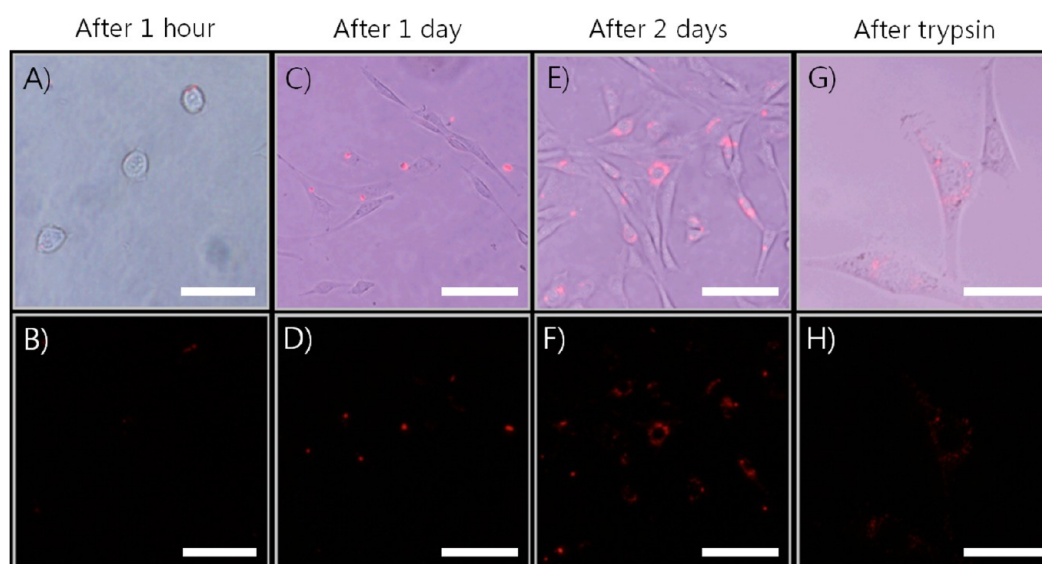


Figure 5. Fluorescence images (bottom) and fluorescence merged phase contrast images (top) of fibroblasts attached to 20% PCDA-RGD liposomes (red) after magnetic separation at time points of 1 h (images (a) and (b), scale bar: 50 μm), 1 day (images (c) and (d), scale bar: 100 μm), and 2 days (images (e) and (f), scale bar: 100 μm). In addition, cells were trypsinized on day 2 and put on a new dish for observation on the following day 3 (images (g) and (h), scale bar: 25 μm).

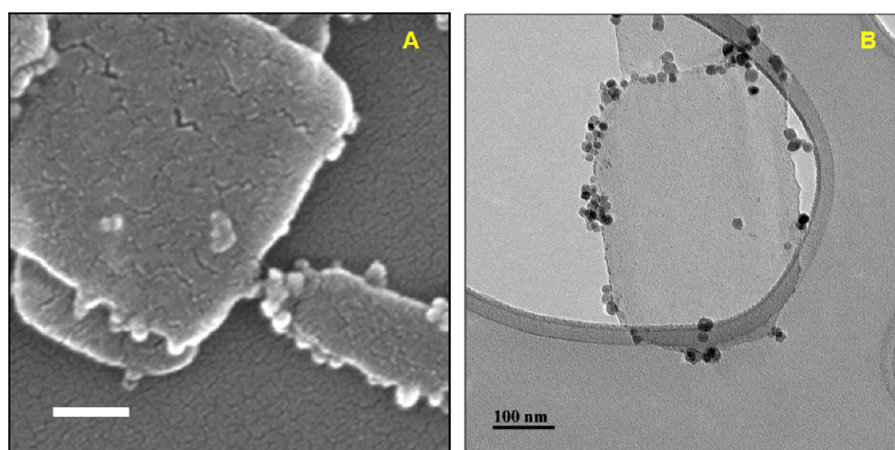


Figure 6. (a) SEM image and (b) TEM image of magnetite-conjugated 20% PCDA-RGD liposomes. (scale bars: 100 nm).

with ligand surface densities above 20% revealed significant steric hindrance as was assessed by the absorbance shift attributed to rotation away from planar π orbital overlap in the PDA backbone. As such, a biomaterial with ligand density of 20% appears significantly different on a molecular level as compared to one with 50% surface density from the perspective of cell–biomaterial interactions. This strong correlation with our results from the cell adhesion study, wherein cell binding decreases for liposomes having greater than 20% ligand density, supports that ligand accessibility and surface density-driven steric effects may block binding access to cellular receptors, such as integrins. Results such as this are of utmost importance for controlling cell adhesion and correspondingly for biomaterials design. Direct control of ligand chemistry and surface density on the liposome via facile self-assembly provides an advantageous means for examining steric hindrance effects within a biomaterial–cell interface. While we have chosen, in this proof of concept, to use RGD motifs as the displayed ligand given its extensive use in cell adhesion studies,³⁴ multiple different ligand motifs may be simultaneously displayed as a

mixture on the liposome surface in order to access not only avidity effects but perhaps cooperativity as well.

The agreement in results between our cell adhesion study and our colorimetric/fluorometric assay strongly supports that this approach can be used to obtain significant information on the interaction between a biomaterial and cell surface. We also show that cells separated magnetically remain adherent to the fluorescent magnetic-liposomes allowing for further study of cell behavior. In our study, liposome-bound cells were imaged with bright-field and fluorescence microscopy 1 h and also 1 day after magnetic isolation. As seen in Figure 4, some cells were already adhering to plates even 1 h after cell separation, and were well-spread by the following day, exhibiting morphology and growth rates characteristic of NIH 3T3 cells. After 1 day of incubation, the magnetic-liposomes were found to remain bound to the surface of the cells (Figure 5). Under these conditions, the magnetic-liposomes appeared to have little effect on cell viability (Supplementary Figure 3 of the SI), and the fibroblasts grew to confluence as normal. After exploring a range of magnetic liposomes concentrations, we

find a gradual reduction in cell growth does occur under incubation at high liposome concentrations (Supplementary Figure 4 of the SI). After 1 h and 1 day, we find, by overlaying fluorescence and phase contrast images, what appears to be the colocalization of the fluorescent magnetic liposomes along the cell edges, consistent with where integrin adhesion complexes are typically found (Figure 5 and Supplementary Figure 7 of the SI). At time points of 1 h and 1 day, the cells were imaged, and the number of liposome-MNP aggregates were quantified using imageJ to build a histogram of the number of particles per cell using three images for each time point. The results (Supplementary Figure 2 of the SI) revealed an average of 4.0 liposome-MNP aggregates per cell after 1 h, while 2.6 liposome-MNP aggregates were observed at 1 day of incubation. Interestingly, after 2 days we can no longer observe the presence of individual fluorescent aggregates only at the cell surface, but rather many smaller and more uniformly spread fluorescent particles could be observed throughout an area resembling the cell cytoplasm (Figure 5). This observation may be a result of endocytosis of individual fluorescent liposomes or fragments that have disassociated from aggregated cluster after several days of incubation, while the larger clusters may be remaining on the cell surface. The leading hypothesis for cell adherence to RGD bearing substrates is that 3T3 cells can recycle adhered $\alpha 5 \beta 1$ integrins through clathrin mediated endocytosis.³⁵ After 2 days, trypsin was added to passage the cells into a new plate, and after growth for an additional third day, we could see fluorescence only in what appeared to be the cytoplasmic space (Figure 5g), rather than limited to the cell surface as seen on day 1. SEM and TEM images of magnetite-conjugated 20% PCDA-RGD liposomes are shown in Figure 6. Future works exploring the intracellular use of these materials may be of interest, while further assessment may also show these biomaterial coated PDA liposomes as having potential use as markers for hot spots of cellular mechanical activity owing to the force responsive nature of PDA fluorescence. The possibility for utilizing cell-specific ligands in combination with this systems fluorescent capability may find additional specialized applications.

The strategy developed here may be used to evaluate the cell adhesivity of polymeric liposomes coated with a wide variety of different adhesion ligands and at various surface densities. This tool may thus be of use in the design of biomaterials with particular cell binding characteristics. Furthermore, the separation technique when used in combination with successive analytical methods may provide information related to processes including modulation of cytoskeletal assembly or the activation of intracellular signaling pathways due to chemical cues arising from the biomaterial interaction.³⁶ As mentioned previously, the chemical cues are but one part of the complex cross-talk occurring at the cell–biomaterial interface, but with this system, performing downstream analyses is a realistic option. Using the magnet-assisted separation step capabilities of this system may offer the isolation of viable bound cells in concentrated samples. One may also envision using this system in a negative screening mode to assess the critical factors or components that inhibit cell–biomaterial or protein–protein interactions. Because these liposomes can be tailored to a variety of combinations of surface chemistries, they will find relevance for a range of research fields, taking on broad interest. We envision that this system may be fitting to researchers studying biomaterials, cell–matrix interactions, and immunology, by providing an easily customizable tool for not

only probing, but also controlling the molecular-level surface features that can play a role in cell adhesivity.

CONCLUSIONS

We present in this work a novel fluorescent liposome conjugated with magnetite found to offer a means for biomaterial screening of cell adhesivity. This material system developed here allows for the controlled display of mixtures of surface chemistries at tunable surface densities. The unique ability to simultaneously assess surface steric affects, due to ligand overcrowding for instance, is achieved by an inherent colorimetric and fluorometric response. By offering a straightforward method for counting of cells bound to the biomaterial of interest after magnet-assisted cell separation, this system provides a measure of cell adhesivity. In our demonstration using the model RGD ligand, we demonstrate that a surface density of 20% RGD provides the best cell adhesion for our PDA liposome system, which is in agreement with other more intricate analytical approaches.³³ In conjunction with fluorescence measurements, we confirm this intermediate surface density provides a suitable balance between ligand density and steric hindrance for cell adhesivity. After magnetic separation, the liposomes were found to provide fluorescent markers that remained bound to the fibroblasts, offering the potential for subsequent analysis. This system may be utilized to screen other combinations of peptide-based ligands to provide a simple method for examining the interplay between steric affects, ligand accessibility, and cell adhesivity.

ASSOCIATED CONTENT

Supporting Information

Full characterization results (DLS and SEM), details on the solid-phase synthesis of PCDA-RGD, cytotoxicity results, liposomal aggregate counting histograms, digitally magnified images of cells after magnetic separation, as well as additional cell adhesion studies using different surface chemistries. This material is available free of charge via the Internet at <http://pubs.acs.org>.

AUTHOR INFORMATION

Corresponding Author

*Tel: +82-(2)-2220-1935; fax: +82-(2)-2220-2339; e-mail: justynj@hanyang.ac.kr.

Author Contributions

The manuscript was written through contributions of all authors. All authors have given approval to the final version of the manuscript.

Notes

The authors declare no competing financial interest.

ACKNOWLEDGMENTS

This work was supported by the Priority Research Centers Program through the National Research Foundation of Korea (NRF) funded by the Ministry of Education, Science and Technology (2012R1A6A1029029), by the research fund of Hanyang University (HY-2011-N), and by the NSF EAPSI grant.

ABBREVIATIONS

RGD, Arginine-Glycine-Aspartate; ECM, Extracellular Matrix; MALDI-TOF, Matrix-Assisted Laser Desorption/Ionization-Time of Flight Mass Spectroscopy

REFERENCES

- (1) Albelda, S. M.; Buck, C. A. Integrins and other cell adhesion molecules. *FASEB J.* **1990**, *4* (11), 2868–2880.
- (2) Ventre, M.; Causa, F.; Netti, P. A. Determinants of cell–material crosstalk at the interface: Towards engineering of cell instructive materials. *J. R. Soc. Interface* **2012**, *9* (74), 2017–2032.
- (3) Humphries, M. Cell adhesion assays. *Mol. Biotechnol.* **2001**, *18* (1), 57–61.
- (4) Cell Adhesion: Protocol Manual. In *BD Biosciences*; Becton, Dickinson and Company: Franklin Lakes, New Jersey, 2001; p 60.
- (5) Aparicio, C. L.; Strong, L. H.; Yarmush, M. L.; Berthiaume, F. Correction for label leakage in fluorimetric assays of cell adhesion. *BioTechniques* **1997**, *23* (6), 1056–1060.
- (6) Bellavite, P.; Andrioli, G.; Guzzo, P.; Arigliano, P.; Chirumbolo, S.; Manzato, F.; Santonastaso, C. A colorimetric method for the measurement of platelet adhesion in microtiter plates. *Anal. Biochem.* **1994**, *216* (2), 444–450.
- (7) Safark, I.; Safarkova, M. Use of magnetic techniques for the isolation of cells. *J. Chromatogr. B: Biomed. Sci. Appl.* **1999**, *722* (1), 33–53.
- (8) Jain, S.; Mishra, V.; Singh, P.; Dubey, P. K.; Saraf, D. K.; Vyas, S. P. RGD-anchored magnetic liposomes for monocytes/neutrophils-mediated brain targeting. *Int. J. Pharm.* **2003**, *261* (1–2), 43–55.
- (9) Fortin-Ripoche, J.-P.; Martina, M. S.; Gazeau, F.; Ménager, C.; Wilhelm, C.; Bacri, J.-C.; Lesieur, S.; Clément, O. Magnetic targeting of magnetoliposomes to solid tumors with MR imaging monitoring in mice: Feasibility 1. *Radiology* **2006**, *239* (2), 415–424.
- (10) Ito, A.; Ino, K.; Kobayashi, T.; Honda, H. The effect of RGD peptide-conjugated magnetite cationic liposomes on cell growth and cell sheet harvesting. *Biomaterials* **2005**, *26* (31), 6185–6193.
- (11) Davis, D. H.; Giannoulis, C. S.; Johnson, R. W.; Desai, T. A. Immobilization of RGD to (111) silicon surfaces for enhanced cell adhesion and proliferation. *Biomaterials* **2002**, *23* (19), 4019–4027.
- (12) Pierschbacher, M. D.; Ruoslahti, E. Cell attachment activity of fibronectin can be duplicated by small synthetic fragments of the molecule. *Nature* **1984**, *309* (5963), 30–33.
- (13) Jung, Y. K.; Park, H. G.; Kim, J.-M. Polydiacetylene (PDA)-based colorimetric detection of biotin–streptavidin interactions. *Biosens. Bioelectron.* **2006**, *21* (8), 1536–1544.
- (14) Sun, X.; Chen, T.; Huang, S.; Li, L.; Peng, H. Chromatic polydiacetylene with novel sensitivity. *Chem. Soc. Rev.* **2010**, *39* (11), 4244–4257.
- (15) Charych, D.; Cheng, Q.; Reichert, A.; Kuziemko, G.; Stroh, M.; Nagy, J. O.; Spevak, W.; Stevens, R. C. A 'litmus test' for molecular recognition using artificial membranes. *Chem. Biol.* **1996**, *3* (2), 113–120.
- (16) Chen, X.; Kang, S.; Kim, M. J.; Kim, J.; Kim, Y. S.; Kim, H.; Chi, B.; Kim, S.-J.; Lee, J. Y.; Yoon, J. Thin-film formation of imidazolium-based conjugated polydiacetylenes and their application for sensing anionic surfactants. *Angew. Chem., Int. Ed.* **2010**, *49* (8), 1422–1425.
- (17) Hsu, L.; Cvetanovich, G. L.; Stupp, S. I. Peptide amphiphile nanofibers with conjugated polydiacetylene backbones in their core. *J. Am. Chem. Soc.* **2008**, *130* (12), 3892–3899.
- (18) Reppy, M. A.; Pindzola, B. A. Biosensing with polydiacetylene materials: Structures, optical properties and applications. *Chem. Commun.* **2007**, *42*, 4317–4338.
- (19) Yarmaga, O.; Jaworski, J.; Yoon, B.; Kim, J.-M. Polydiacetylenes: Supramolecular smart materials with a structural hierarchy for sensing, imaging and display applications. *Chem. Commun.* **2012**, *48* (19), 2469–2485.
- (20) Biesalski, M.; Tu, R.; Tirrell, M. V. Polymerized vesicles containing molecular recognition sites. *Langmuir* **2005**, *21* (13), 5663–5666.
- (21) Jaworski, J.; Yokoyama, K.; Zueger, C.; Chung, W.-J.; Lee, S.-W.; Majumdar, A. Polydiacetylene incorporated with peptide receptors for the detection of trinitrotoluene explosives. *Langmuir* **2011**, *27* (6), 3180–3187.
- (22) Scindia, Y.; Silbert, L.; Volinsky, R.; Kolusheva, S.; Jelinek, R. Colorimetric detection and fingerprinting of bacteria by glass-supported lipid/polydiacetylene films. *Langmuir* **2007**, *23* (8), 4682–4687.
- (23) Biesalski, M. A.; Knaebel, A.; Tu, R.; Tirrell, M. Cell adhesion on a polymerized peptide–amphiphile monolayer. *Biomaterials* **2006**, *27* (8), 1259–1269.
- (24) Kwon, I. K.; Song, M. S.; Won, S. H.; Choi, S. P.; Kim, M.; Sim, S. J. Signal amplification by magnetic force on polydiacetylene supramolecules for detection of prostate cancer. *Small* **2012**, *8* (2), 209–213.
- (25) Chen, X.; Li, L.; Sun, X.; Liu, Y.; Luo, B.; Wang, C.; Bao, Y.; Xu, H.; Peng, H. Magnetochromatic polydiacetylene by incorporation of Fe₃O₄ nanoparticles. *Angew. Chem., Int. Ed.* **2011**, *50* (24), 5486–5489.
- (26) Lee, J.; Yoon, B.; Ham, D.-Y.; Yarmaga, O.; Lee, C. W.; Jaworski, J.; Kim, J.-M. Magnetically responsive inorganic/polydiacetylene nanohybrids. *Macromol. Chem. Phys.* **2012**, *213* (9), 893–903.
- (27) Jun, Y.-w.; Seo, J.-w.; Cheon, J. Nanoscaling laws of magnetic nanoparticles and their applicabilities in biomedical sciences. *Acc. Chem. Res.* **2008**, *41* (2), 179–189.
- (28) Kim, D.; Lee, N.; Park, M.; Kim, B. H.; An, K.; Hyeon, T. Synthesis of uniform ferrimagnetic magnetite nanocubes. *J. Am. Chem. Soc.* **2008**, *131* (2), 454–455.
- (29) Park, J.; An, K.; Hwang, Y.; Park, J.-G.; Noh, H.-J.; Kim, J.-Y.; Park, J.-H.; Hwang, N.-M.; Hyeon, T. Ultra-large-scale syntheses of monodisperse nanocrystals. *Nat. Mater.* **2004**, *3* (12), 891–895.
- (30) Kim, J.-M.; Park, B.; Chang, E.-J.; Yi, S.; Suh, D.; Ahn, D. The solid-phase synthesis of amino acid-derived diacetylene lipids. *Macromol. Res.* **2005**, *13* (3), 253–256.
- (31) Corr, S. A.; O'Byrne, A.; Gun'ko, Y. K.; Ghosh, S.; Brougham, D. F.; Mitchell, S.; Volkov, Y.; Prina-Mello, A. Magnetic-fluorescent nanocomposites for biomedical multitasking. *Chem. Commun.* **2006**, *0* (43), 4474–4476.
- (32) Son, H.; Lee, J. H.; Kim, Y.-R.; Lee, I. S.; Han, S.; Liu, X.; Jaworski, J.; Jung, J. H. A BODIPY-functionalized bimetallic probe for sensitive and selective color-fluorometric chemosensing of Hg²⁺. *Analyst* **2012**, *137* (17), 3914–3916.
- (33) Dillo, A. K.; Ochsenhirt, S. E.; McCarthy, J. B.; Fields, G. B.; Tirrell, M. Adhesion of $\alpha 5\beta 1$ receptors to biomimetic substrates constructed from peptide amphiphiles. *Biomaterials* **2001**, *22* (12), 1493–1505.
- (34) Hersel, U.; Dahmen, C.; Kessler, H. RGD modified polymers: Biomaterials for stimulated cell adhesion and beyond. *Biomaterials* **2003**, *24* (24), 4385–4415.
- (35) Ezratty, E. J.; Bertaux, C.; Marcantonio, E. E.; Gundersen, G. G. Clathrin mediates integrin endocytosis for focal adhesion disassembly in migrating cells. *J. Cell Biol.* **2009**, *187* (5), 733–747.
- (36) Humphries, M. J. Cell adhesion assays. *Methods Mol. Biol.* **2009**, *522*, 203–10.